Dielectric Properties and Solubility of Multilayer Hyperbranched Polyimide/Polyhedral Oligomeric Silsesquioxane Nanocomposites

Bongkoch Somboonsub, Supakanok Thongyai, Piyasan Praserthdam

Center of Excellence on Catalysis and Catalytic Reaction Engineering, Department of Chemical Engineering, Faculty of Engineering, Chulalongkorn University, Bangkok 10330, Thailand

Received 31 May 2008; accepted 5 April 2009
DOI 10.1002/app.30663
Published online 7 August 2009 in Wiley InterScience (www.interscience.wiley.com).

ABSTRACT: Multilayer hyperbranched polyimide/polyhedral oligomeric silsesquioxane (POSS) nanocomposites were synthesized by the reaction of a bromide-hyperbranched polyether/POSS and a main-chain polyimide containing hydroxyl-functional groups. The first layer was formed through the direct reactions of the main-chain hydroxyl groups with monochloroisobutyl polyhedral oligomeric silsesquioxane (POSS–Cl). The second and third layers were prepared by the repeated reactions of bromine ether branches that incorporated POSS–Cl with 3,5-dihydroxybenzyl alcohol. Regardless of the fixed amount of POSS, the higher layers yielded lower dielectric constants. Even when the amount of the POSS loading was reduced 4-fold, the third layer still had the lowest dielectric constants. The lowest dielectric constant of 2.54 was found in the third layer of the hyperbranched polyimide/POSS nanocomposite because of the large free volume and loose polyimide structures. The densities of the hyperbranched polyimide/POSS nanocomposite corresponded to the dielectric constants. The lower the density was, the higher the free volume was and the lower the dielectric constant was. The experimental results indicated that the hyperbranched polyimide/POSS nanocomposite exhibited increased solubility in comparison with pure polyimide. J Appl Polym Sci 114: 3292–3302, 2009

Key words: hyperbranched; nanocomposites; polyimides; synthesis

INTRODUCTION

The first commercial polyimide film was introduced by DuPont in the 1960s because of its excellent thermooxidative stability, high mechanical strength, high modulus, superior chemical resistance, excellent electrical properties, low dielectric constant, low relative permittivity, inertness to solvents, good adhesion properties, and high thermal stability. Aromatic polyimides are widely used in electronics and aerospace applications.[1] The development of polyimides for electronics has been focused primarily on the role of the chemical structure in providing desired properties such as a low dielectric constant and high thermomechanical stability. Therefore, polyimide is a polymer with a very low dielectric constant (3.5).

One of the developments in low-dielectric-constant polymers is increased free volume in the structure. The incorporation of a silica cage such as polyhedral oligomeric silsesquioxane (POSS) into the polyimide matrix has been widely investigated.[2–6] A hybrid nanomaterial of POSS combines unique inorganic–organic chemical compositions with nanosized cage structures. The incorporation of POSS cages into polymeric materials often results in many improvements in polymer nanocomposite properties such as temperature and oxidation resistance and dielectric and mechanical properties.[7] Transmission electron microscopy images of POSS nanocomposites can be found in the literature.[8]

Recently, dendritic macromolecules have attracted considerable attention because of their unique structures.[9] They are mainly classified into dendrimers with well-defined structures and hyperbranched polymers with statistically branched architectures. Although the synthesis of such structures requires many reaction steps, hyperbranched polymers can be prepared by one-step polymerization of monomers and seem to be suitable for large-scale production. In comparison with their linear analogues, hyperbranched polymers possess good solubility in organic solvents and decreased viscosity and interchain entanglement. In addition, various functional groups can be introduced into their structures to create new functional polymeric materials.

In this work, multilayer hyperbranched polyimide/POSS nanocomposites synthesized by the incorporation of POSS into the side chains of

Correspondence to: S. Thongyai (tsupakan@chula.ac.th).
Contract grant sponsor: Thailand Research Fund, Graduate School at Chulalongkorn University.

polyimide were examined for the first time. Monochloroisobutyl polyhedral oligomeric silsesquioxane (POSS–Cl) was directly attached to the hydroxyl main chain of polyimide in the first layer of the nanocomposite. By repeated reactions of a bromoether branch incorporating POSS–Cl with 3,5-dihydroxybenzyl alcohol (DA), the second and third layers of the hyperbranched polyether nanocomposite were formed. The solubility, density, and dielectric properties of this new type of nanocomposite were investigated as a function of the POSS loading. Proton nuclear magnetic resonance (^{1}H-NMR) and Fourier transform infrared (FTIR) were also used to indicate the structure of the obtained nanocomposite.

EXPERIMENTAL

Materials

All reactions and polymerizations were manipulated under an argon atmosphere with a glovebox and/or Schlenk techniques. 4,4′-(Hexafluoroisopropylidene) diphthalic anhydride (6FDA; Aldrich Chemical Co., Inc., USA), 3,4′-oxydianiline (ODA; Aldrich Chemical), 3,3′-dihydroxy-4,4′-diamino biphenyl (DHBP; Chriskev Co., Inc., USA), and phthalic anhydride (PA; Merck KGaA, Germany) were used without additional purification. *N*-Methyl-2-pyrrolidinone (NMP; Merck, Germany) was the solvent used in polyimide synthesis. POSS–Cl was obtained from Hybrid Plastic Co. DA was purchased from Aldrich Chemical, and potassium carbonate (K_2CO_3), carbon tetrabromide (CBr_4; Merck), and triphenylphosphine (PPh_3; Aldrich Chemical) were used for the synthesis of hyperbranched ether. Toluene, methanol, acetone, and tetrahydrofuran (THF) were obtained from Merck.

Polyimide polymerization

Various hydroxyl concentrations of polyimide capped with nonreactive end groups were prepared by the reaction of 6FDA with diamine mixtures of DHBP and ODA in NMP, and they were further capped with PA. The content of hydroxyl groups in the polyimide was controlled by adjustments of the molar ratio of the diamine monomers (DHBP and ODA). Here, synthesized polyimides with 25, 50, 75, and 100% DHBP in the total diamine mixtures are coded as PI25, PI50, PI75, and PI100, respectively.

As a typical example, the preparation of PI50 can be explained as follows. A three-necked, round-bottom flask equipped with a purified argon inlet, a thermometer, a magnetic stirring bar, and a condenser with a Dean–Stark trap was used as the reaction vessel. DHBP (1.5039 mmol, 0.3248 g), ODA (1.5039 mmol, 0.3008 g), and 6 mL of NMP were added to a reaction vessel. The mixture was stirred at the ambient temperature until both diamines were completely dissolved. Next, 6FDA (3.0000 mmol, 1.3326 g) with NMP was added to the solution to obtain about 10% (w/w) solids. The solution was stirred under an argon atmosphere for 8 h at room temperature. Subsequently, PA (0.0154 mmol, 0.0023 g) was added to the solution with stirring for another 4 h to obtain PA-end-capped poly(amic acid) (PAA). Toluene (20 mL) was added to the reaction solution to remove water from the condensation polymerization by azeotropic distillation for approximately 20 h at 180°C. After cooling, the solution was precipitated in 500 mL of a 1 : 1 methanol/deionized water mixture. The precipitated polyimide was filtered and dried in a vacuum oven at 150°C for 15 h, and the PI50 obtained was kept for further grafting with hyperbranched polyethers.

Preparation of one to three layers of hyperbranched polyether on polyimide

Preparation of the first layer (PI50–L1)

A mixture of POSS–Cl in THF and a polyimide (PI50) in an NMP solution were stirred for 3 h to obtain a POSS/polyimide composite, which was coded as PI50–L1. The obtained solution was directly cast into a film shape on a clean glass plate, and the remaining solvent was evaporated *in vacuo* at 50°C for 10 h. The cast films were thermally treated at 100°C (1 h) and at 150 and 200°C (0.5 h each) in a temperature-controlled oven. After the thermal treatment, the films were removed from the glass substrate by immersion into water and dried at 100°C for 24 h.

Preparation of the second layer (PI50–L2)

Synthesis of dendritic benzyl alcohols ([G-1]OH, first layer of dendritic benzyl alcohols). A mixture of the appropriate POSS–Cl (2.00 equiv), DA (1.00 equiv), and dried K_2CO_3 (2.50 equiv) in dry toluene/acetone was heated, refluxed, and stirred vigorously under an argon atmosphere for 48 h. The mixture was dried by cooling and evaporation of the remaining solvent. The residual product was washed with deionized water three times and further dried in a vacuum oven at 100°C for 3 h.

Synthesis of dendritic benzyl bromides ([G-1]Br, first layer of dendritic benzyl bromides). The appropriate [G-1]OH (1.00 equiv) and CBr_4 (1.25 equiv) were dissolved in THF. Next, PPh_3 (1.25 equiv) was added, and the reaction mixture was stirred under argon for 1 h. The solvent was evaporated completely from the solution. The dry residue ([G-1]Br) was washed with

acetone three times before being dried in a vacuum oven at 67°C for 3 h.

Second layer of the branched polyether-grafted polyimide (PI50–L2). The polyimide (PI50) was dissolved in NMP to produce a 15% solution, whereas [G-1]Br was separately dissolved in THF to produce a 15% solution. Then, the [G-1]Br solution was slowly poured into the polyimide solution and stirred for 3 h. The obtained solution was directly cast into a film shape on a clean glass plate. The remaining solvent was evaporated *in vacuo* at 50°C for 10 h. The cast film of PI50–L2 was thermally treated at 100°C (1 h) and at 150 and 200°C (0.5 h each) in a temperature-controlled oven.

Preparation of the third layer (PI50–L3)

Synthesis of the dendritic benzyl alcohols ([G-2]OH, second layer of dendritic benzyl alcohols). The dendritic benzyl alcohols were prepared from [G-1]Br, DA, and dried potassium in dry THF. The obtained mixture was further cooled and evaporated to dryness. The residue of [G-2]OH was washed with deionized water three times and dried in a vacuum oven at 100°C for 3 h.

Synthesis of the dendritic benzyl bromides ([G-2]Br, second layer of dendritic benzyl bromides). The same procedure used for [G-1]Br was employed, except that [G-2]OH was used instead of benzyl alcohol to synthesize [G-2]Br.

Third layer of the branched polyether-grafted polyimide (PI50–L3). With the same procedure used for PI50–L2, PI50–L3 was synthesized. All the hyperbranched polyimide/POSS nanocomposites were synthesized with similar procedures.

Characterization of the nanocomposite

IR spectra were recorded with a Nicolet 6700 FTIR spectrometer (USA) with a scanning range of 400–4000 cm^{-1} with 64 scans at a resolution of 4 cm^{-1}.

^{1}H-NMR spectra of the polymer were obtained on a Bruker Biospin DPX400 NMR spectrometer (Switzerland) operating at 400 MHz in hexadeuterated dimethyl sulfoxide with tetramethylsilane as an internal standard, and the number of scans was 32.

The inherent viscosities of polyimide solutions in NMP were measured with an Ubbelohde viscosimeter at 40°C, and the molecular weights of the polyimides were calculated from the obtained intrinsic viscosities. Calibration with standard polystyrene was also performed.

The dielectric properties of the polyimide films were obtained via the capacitance method and were measured at room temperature at 500 mV with an Agilent E 4980A precision LCR meter (USA). The 1.5 × 1.5 cm^2 films for dielectric property analysis were coated with a gold layer with a JEOL JFC-1100E ion-sputtering device (USA) on both sides to provide electrical contact with the specimens before the measurements.

The densities were measured from the weight of the polyimide films over the volume of the specimens of known dimensions (1.5 cm × 1.5 cm × thickness = volume).

The surface morphology was recorded in the tapping mode of an atomic force microscopy (AFM) system (Nanoscope IV, USA) by silicon probe tips at the resonance frequency of 204–497 kHz.

To classify the solubility of the hyperbranched polyimide, 0.1 g of the polyimide was dissolved in various solvents (0.9 g) at room temperature.

RESULTS AND DISCUSSION

Preparation of the polymer

Preparation of the polyimide (PI50–L0)

PAA was synthesized by the reaction between 6FDA, 3,4′ODA, and DHBP and end-capped by PA in aprotic solvents to obtain various hydroxyl-functional groups. PAA was further *in situ* one-step imidized by the azeotropic distillation of toluene to remove water from imide condensation polymerization. The polyimide product could be obtained in solution because of the solubility of 6FDA, which was chosen as a dianhydride to produce the soluble polyimide.[10] The soluble products were needed for further reactions with the soluble hyperbranched polyethers. The content of the hydroxyl-functional groups could be varied by changes in the ratio of DHBP to ODA while the ratio of dianhydride to diamine was kept equal to 1 : 1. The resultant polyimide after imidization is shown in Scheme 1. The FTIR spectra, shown in Figure 1, indicated the complete imidization of the polyimide.

In Figure 1, the characteristic peaks of the imide groups can be observed at 1785 cm^{-1} for C=O asymmetric stretching vibrations, at 1720 cm^{-1} for C=O symmetric stretching vibrations, at 1380 cm^{-1} for C—N stretching vibrations, and at 725 cm^{-1} for C=O bending vibrations. The carbonyl group (C=O) in the CONH stretching band around 1660 cm^{-1} disappears in Figure 1, and this indicates the complete imidization of the polyimide. The broad absorption around 3400 cm^{-1} can be attributed to hydroxyl groups contained in the main chains because of the cooperation of DHBP.

Preparation of the first layer (PI50–L1)

POSS–Cl was directly reacted with reactive hydroxyl groups of the polyimide. The concentrations of hydroxyl groups in the polyimide could be adjusted by the synthesis ratio of the diamine monomers DHBP (which contained two hydroxyl groups per

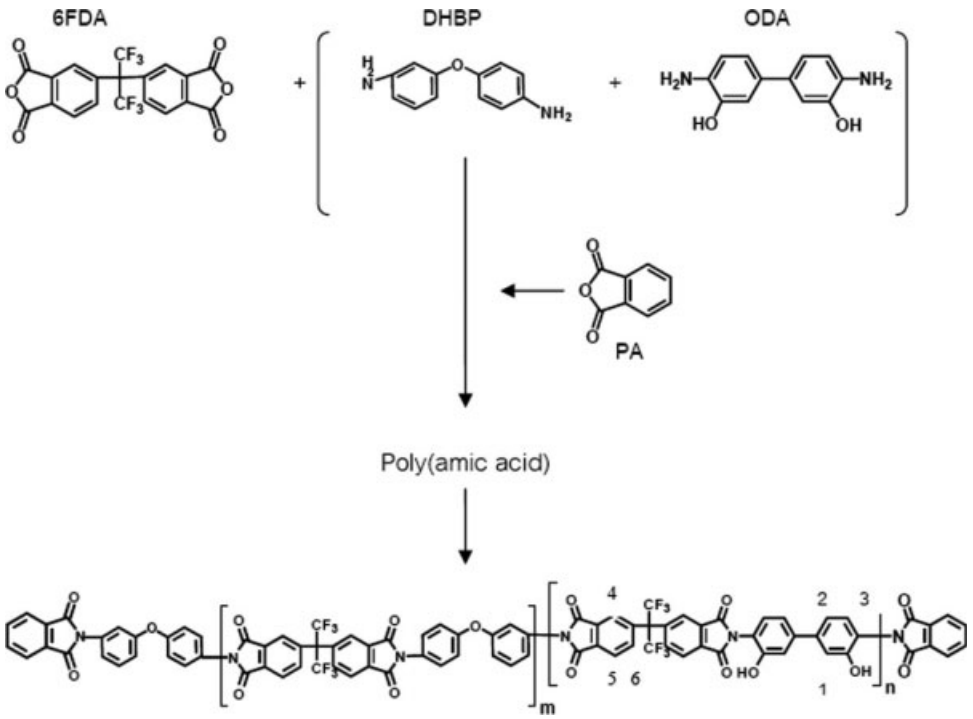

Scheme 1 Structure of the polyimide.

molecule) and ODA (which contained no hydroxyl groups). The amount of POSS was kept constant at 10% of the hydroxyl-functional groups of the polyimide. In other words, the molar ratio of OH to POSS was kept constant at 1 : 0.1. The polyimide/POSS nanocomposites are shown in Scheme 2.

In Figure 1, the FTIR spectra of the first layer of the hyperbranched polyimide/POSS nanocomposite and pure polyimide before cooperation with POSS–Cl can be compared. Confirming the cooperation of POSS–Cl with the polyimide, the FTIR spectrum of the cooperated polyimide shows the

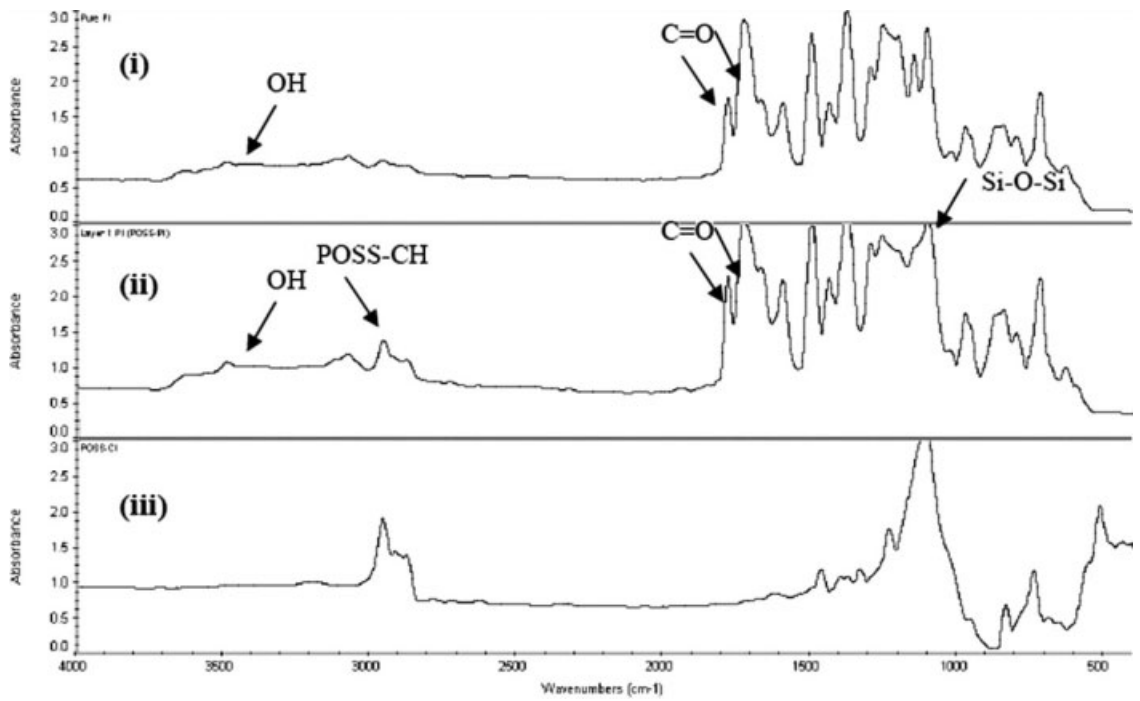

Figure 1 FTIR spectra of (i) the pure polyimide, (ii) POSS/polyimide (first layer), and (iii) POSS–Cl.

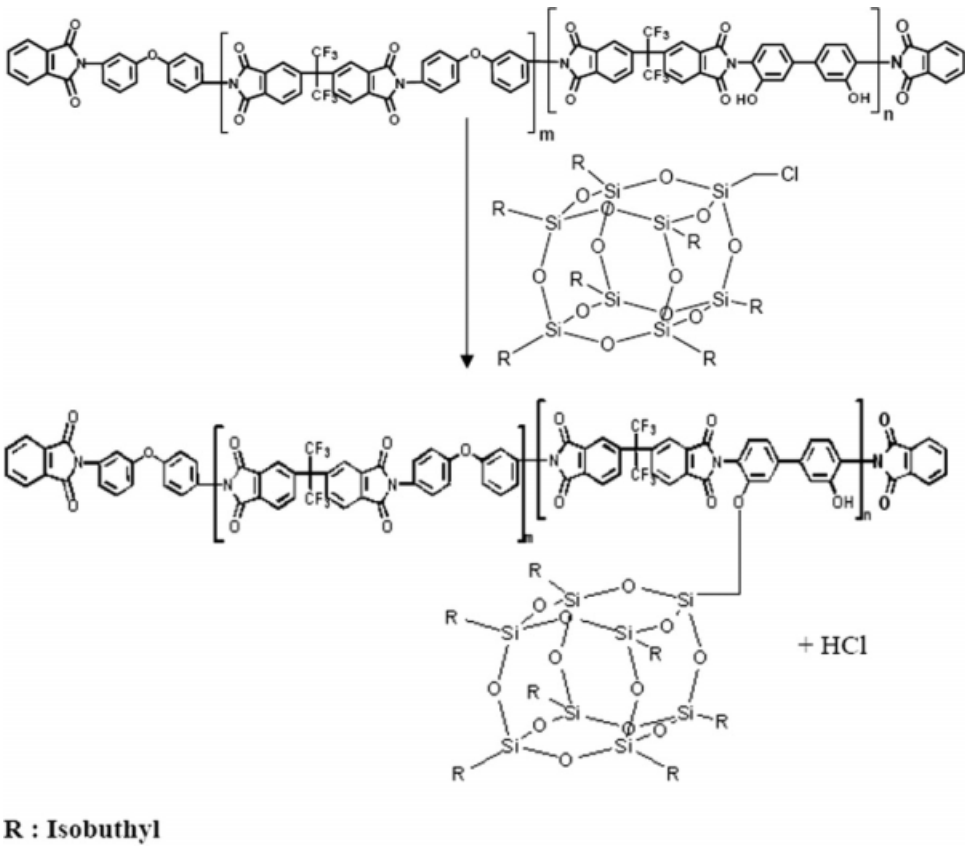

Scheme 2 Structure of POSS/polyimide (first layer).

peaks of the functional groups representing the Si—O—Si asymmetric stretching absorption between 1000 and 1180 cm^{-1} and the aliphatic C—H stretching band between 2800 and 2900 cm^{-1}. These characteristic peaks indicate that POSS molecules were incorporated into the side-chain space of the polyimide via the hydroxyl group of DHBP.

Preparation of the second layer (PI50–L2)

The second layers of the hyperbranched polyimide/POSS nanocomposite were made from the pure polyimide with the readymade hyperbranched ether. The Br-functional groups of the hyperbranched ether ([G-1]Br) reacted with the hydroxyl group of the polyimide and emitted HBr while leaving the oxygen as an ether bond between the ether branch and polyimide. The ether could be synthesized with DA with the POSS–Cl at a molar ratio of 1 : 2. However, DA had three hydroxyl groups; two groups were attached directly to the benzene ring, and the last hydroxyl group was attached with —CH_2—, which was further directly attached to the benzene ring. The two more reactive hydroxyl groups of DA reacted with POSS–Cl and emitted 2 mol of HCl. Usually, the dihydroxyl attached to the benzene ring was much more reactive, so the last hydroxyl group attached to the —CH_2— benzene group was left unreacted. The last hydroxyl group of DA further reacted with CBr_4 and PPh_3 and yielded the Br-functional group instead of the hydroxyl group of the ether. These Br-functional groups, which further reacted with the hydroxyl group of the polyimide, created the hyperbranched structure and emitted HBr (Scheme 3). In other words, one hydroxyl of the polyimide was attached to the ether bond linked between the benzene ring of the main chain and the —CH_2— benzene ring linked to the ether and two POSS molecules.

Preparation of the third layer (PI50–L3)

Instead of the reaction of the ether branch in the second layer ([G-1]Br) with the polyimide main chain, the Br second layer of the branch reacted with DA again. By the same chemical method explained previously, the third layer of the branch ether could be made. Four POSS molecules were attached to the two layers of DA, and the last hydroxyl group of DA was further reacted with CBr_4 and PPh_3 and changed into Br. The Br ether branches obtained ([G-2]Br) were finally attached to the hydroxyl at the polyimide main chain (Scheme 4). In other words, the four POSS–Cl molecules were attached to the

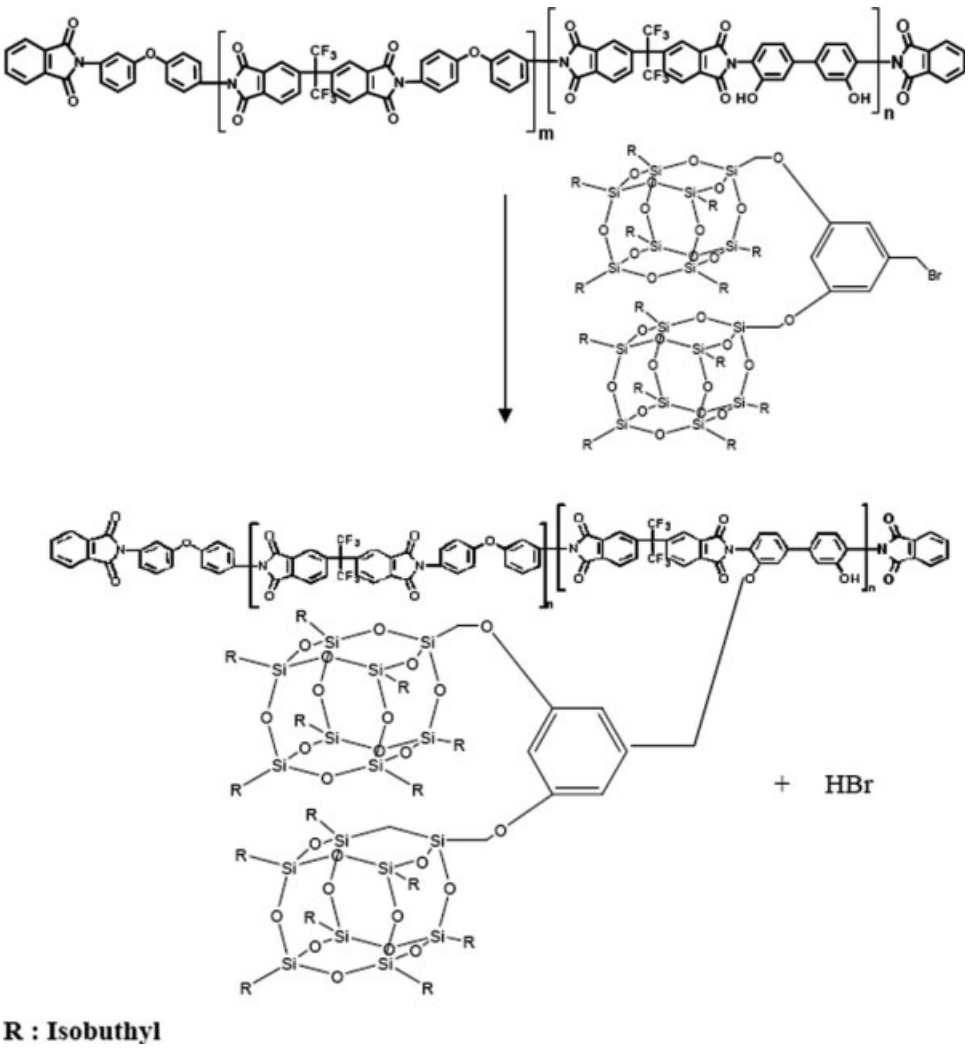

Scheme 3 Structure of the hyperbranched polyimide (second layer).

ether and benzene ring, which were still attached to the ether and other benzene ring before the ether linkage was attached to the main-chain polyimide.

Figure 2(A) shows ^{1}H-NMR spectra of PI50–L0; the resonance peaks at 8.10, 7.95, and 7.90 ppm are assigned to the aromatic protons (4, 5, and 6) of the 6FDA moieties, and the peaks at 7.39, 7.21, and 7.18 ppm are attributed to the aromatic protons (1, 2, and 3) of the DHBP moieties. Figure 2(B) shows ^{1}H-NMR spectra of PI50–L3; the peaks for protons 1a, 2a, and 3a of the dihydroxybiphenyl moieties are shifted downfield to 7.2–7.3 ppm, and this implies the overwhelming existence of covalently tethered POSS and a hyperbranched polyimide/POSS nanocomposite attached to the dihydroxybiphenyl. The resonance peaks in the vicinity of 3.5 ppm (in dimethyl sulfoxide), corresponding to the hydrogen in the benzene ring —CH_2—Br, are not found in Figure 2(A,B). δ_{OH} at 9.3 shifted to 10 in the ^{1}H-NMR spectra from pure polyimide to the hyperbranched polyimide/POSS nanocomposite, and this indicated the overwhelming cooperation of POSS–Br with the OH groups of the polyimide.

When the integration of all the protons (H) in the benzene ring was set equal to 1, the reduction in the ratio of the hydroxyl —OH proton shift at 10 ppm to the nearly constant shift of the proton in the benzene ring around 8–7 ppm in the ^{1}H-NMR spectra of the hyperbranched polyimide/POSS nanocomposite, in comparison with the pure polyimide, confirmed the cooperation of POSS–Br with the OH groups in the case of the hyperbranched polyimide/POSS nanocomposite. In other words, the reduction in OH of the pure polyimide was observed by ^{1}H-NMR; that integration of OH was reduced from 0.069 to 0.014 in comparison with the integration of H in the benzene ring (1.000). The FTIR spectrum of PI50–L3 still showed the OH functions of the polyimide left from the reaction with Br of the branches, and this was confirmed by the ^{1}H-NMR results.

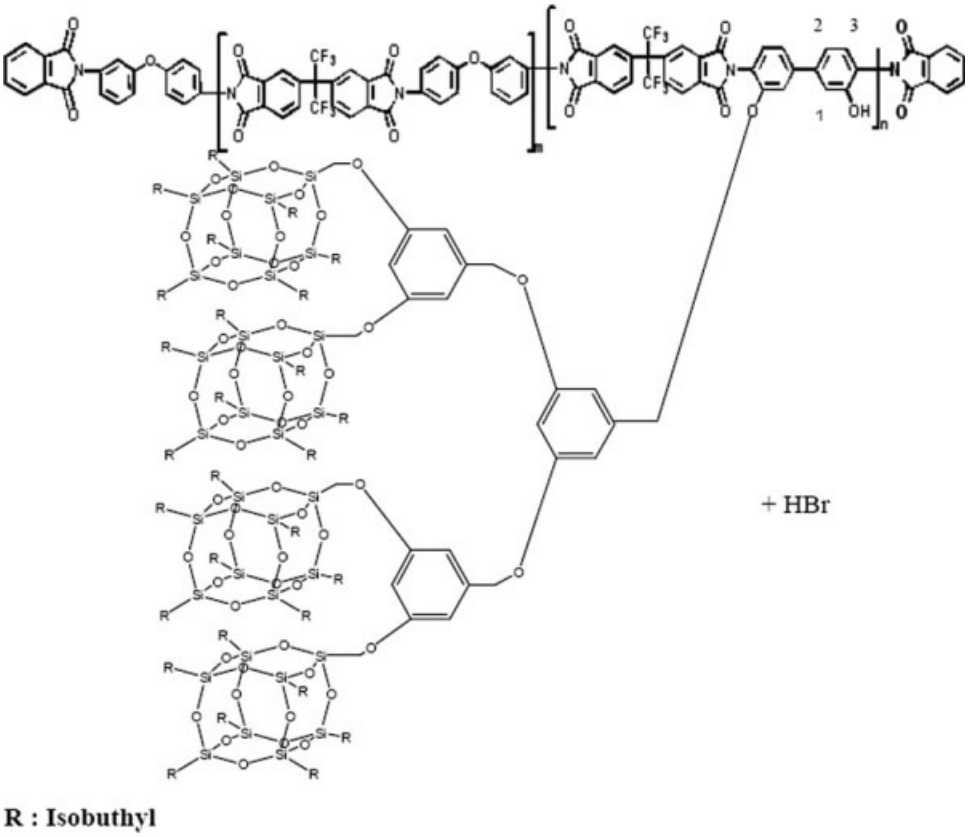

Scheme 4 Structure of the hyperbranched polyimide (third layer).

Viscosities and molecular weights of the polyimide and hyperbranched polyimide/POSS nanocomposites

In Table I, the molecular weights of the polyimide and hyperbranched polyimide/POSS nanocomposite can be rechecked with the solution viscosities of these polymers. The values of the intrinsic viscosity and viscosity-average molecular weight (M_v) of the polyimide and hyperbranched polyimide/POSS nanocomposite are summarized in Table I. The molecular weights of the polyimide increased when the amount of branching increased. Furthermore, in comparison with the results for the viscosity-measured molecular weight (M_v) and stoichiometrically calculated molecular weight, the calculated M_v values were higher than the measured M_v values, regardless of the number of layers. Moreover, the calculated M_v values increased more rapidly than the measured M_v values as the number of layers increased. Dendrimer systems with spherically shaped molecules might have inhibited the extra reduction in viscosity, which finally affected the measured M_v values. The solubility was measured in various solvents such as NMP, dimethylacetamide (DMAc), *m*-cresol, and $CHCl_3$ at room temperature. The solubility properties of the pure polyimide and hyperbranched polyimide/POSS nanocomposite depended on the higher branches and denser molecular structures with the larger number of surface groups. The loose structure was easily dissolved in various solvents (both polar aprotic solvents and normal solvents). For the intrinsic viscosities, the molecular weights of the pure polyimide and hyperbranched polyimide/POSS nanocomposite were measured in only the solvent NMP at 40°C. It was found that the intrinsic viscosities and molecular weights had the same tendency. The increase in the intrinsic viscosities and molecular weights of the polyimide can be explained in terms of increases in the size and branch structure. There are a few possible causes for the increasing viscosities due to the entanglement of chains of the hyperbranched polyimide/POSS nanocomposite, so the third layer of the polyimide had intrinsic viscosities and molecular weights greater than those of the pure polyimide, the first layer, and the second layer.

Dielectric properties of the polyimide and hyperbranched polyimide/POSS nanocomposites

A lower dielectric constant is one of the most desirable properties for the next generation of electronic insulation materials. The dielectric constants of various layers of hyperbranched polyimides are shown

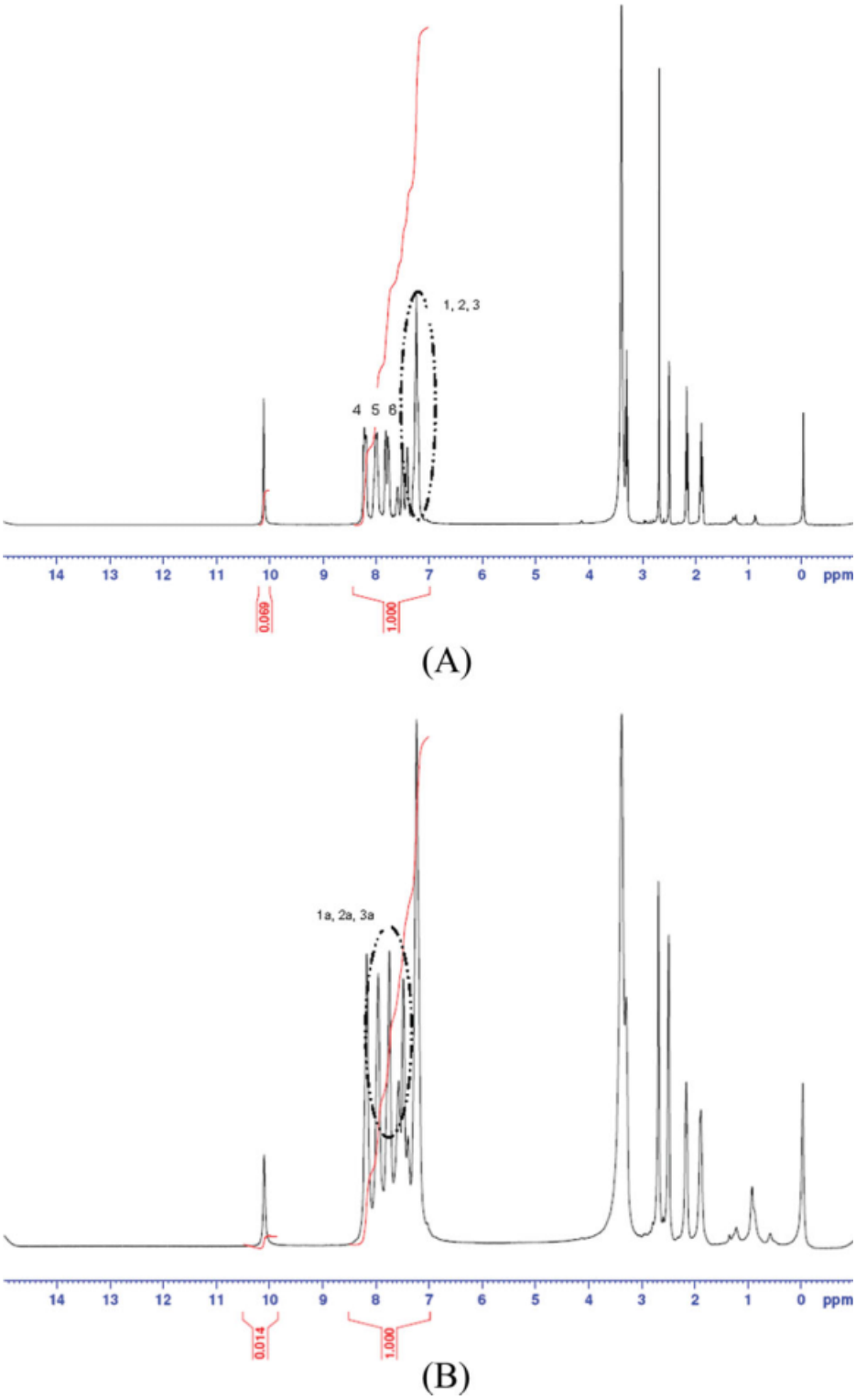

Figure 2 ^{1}H-NMR spectra of (A) the pure polyimide and (B) PI50–L3. [Color figure can be viewed in the online issue, which is available at www.interscience.wiley.com.]

in Table II. The same tendency of POSS increasing and the dielectric constant decreasing can be applied in all layers [layer 1 (L1), layer 2 (L2), and layer 3 (L3)]. Because the ratio of the occupied hydroxyl group of the polyimide to the available hydroxyl in the molecules was kept constant, the higher percentage of the hydroxyl group (PI25 < PI50 < PI75 < PI100) of the hyperbranched polyimide/POSS nanocomposites in the same layer (L1, L2, or L3, respectively) meant more POSS per molecule of the

TABLE I
Viscosities and Molecular Weights of the Polyimide and Hyperbranched Polyimide

Sample	Intrinsic viscosity[a]	Measured M_v	Calculated M_v
PI50–L0	1.3833	86,728	240,000
PI50–L1	1.7072	111,297	366,147
PI50–L2	2.3649	163,787	505,236
PI50–L3	3.0343	220,098	787,625

[a] Measured at 40°C in the solvent NMP.

polyimide. In other words, the more POSS was incorporated, the lower the dielectric constant was, regardless of the amount of the layer applied. The reduction in the dielectric constant by POSS resulted from the low dielectric constant (2.1) of POSS molecules and the higher free volume obtained by the incorporation of POSS into the main-chain polyimide.

The amount of POSS in the nanocomposite could not be overloaded because an overloaded nanocomposite could not be formed as a film (cracked film). Therefore, we strictly used 10% of the hydroxyl (OH) in the main chain in the first layer to react with POSS–Cl in various polyimides (PI25, PI50, PI75, and PI100). In other words, in the first layer of PI25, PI50, PI75, and PI100, there was a maximum POSS branch concentration of 2.5, 5, 7.5, or 10%, respectively. Moreover, we used only half of the POSS in the first layer that cooperated with the second layer of the nanocomposite, regardless of the double amount of POSS per Br contact ([G-1]Br). We used only half of the POSS in the second layer that cooperated with the third layer of the nanocomposite, regardless of the 4-fold amount of POSS per Br contact ([G-2]Br). Thus, in Table III, the total amount of POSS in each layer is summarized.

As shown in Table III, with the same number of hydroxyl groups, the amount of POSS in the first layer was twice that in the second layer, and the amount of POSS in the second layer was twice that in the third layer. In other words, the amount of POSS with the same number of hydroxyl groups (PI25, PI50, PI75, or PI100) was reduced by half in each layer (L1 < L2 < L3). As shown in Table III, the dielectric properties of PI50 in different layers were compared. The third layer had the lowest dielectric constant, the dielectric constant of the second layer was higher than that of the third layer but still lower than that of the first layer, and the first layer had the highest dielectric constant. In other words, the higher the layer number was, the lower the dielectric constant was. Figure 3 shows the dielectric properties versus the amount of POSS in the samples. With the same amount of POSS in various layers, the difference in the dielectric constant of each layer should have come from the difference in the branches. These various layers might have created more free volume in the samples, and the more free volume there was, the lower the dielectric constants were. Moreover, even the number of POSS molecules decreased 4 times in comparison with the first layer, so the third layer had a lower dielectric constant in comparison with the first layer. As shown in Figure 3, the points at the left of the curves of each layer (L1, L2, and L3) represent PI25, and the following points represent PI50, PI75, and PI100 consecutively, regardless of the curve of the layers. For example, for the PI–L1 curve, the left point represents PI25–L1, and the adjacent point represents

TABLE II
Dielectric Constants of the Polyimide Films

Code	Dielectric constant at 1 MHz			
	L0	L1	L2	L3
PI25	3.17	3.13	3.08	2.81
PI50	3.22	3.09	2.88	2.54
PI75	3.40	3.17	3.04	2.73
PI100	3.55	3.16	2.99	2.63

TABLE III
Content of POSS–Cl in the Polyimide and Hyperbranched Polyimide

Code	POSS in the polyimide		Dielectric constant
	mol	wt %	
PI50–L0	0	0	3.22
PI50–L1	3.247×10^{-5}	15.2	3.09
PI50–L2	1.624×10^{-5}	7.6	2.88
PI50–L3	8.113×10^{-6}	3.8	2.54

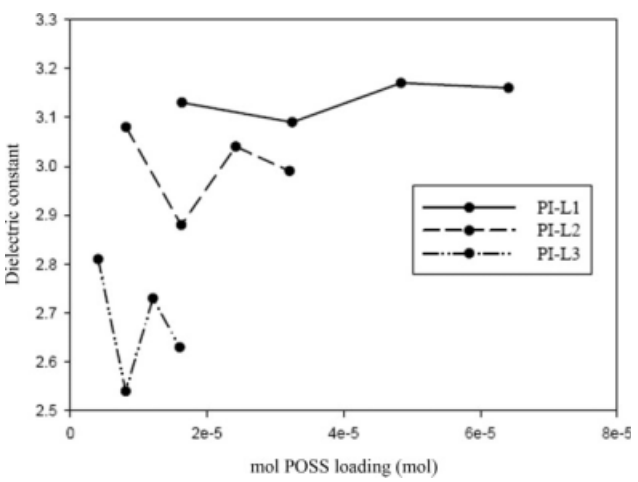

Figure 3 Loading percentage of POSS for various layers and dielectric constants with PI25, PI50, PI75, and PI100 in each layer consecutively from left to right.

TABLE IV
Specific Densities of the Polyimide Films

	Density			
Code	L0	L1	L2	L3
PI25	1.44	1.37	1.28	1.26
PI50	1.43	1.32	1.25	1.19
PI75	1.43	1.34	1.27	1.23
PI100	1.42	1.34	1.23	1.20

PI50–L1, whereas the two points on the right represent PI75–L1 and PI100–L1 consecutively.

The mechanism for the reduction of the dielectric constant can be implied by their densities. As shown in Table IV, the densities of the lower dielectric constant samples in this research were lower. The first assumption comes from the POSS characteristics. The higher POSS molecule inserted the free volumes in the samples, and the dielectric constant and the density also dropped. The second assumption comes from the branch characteristics. The larger sizes of the branches created even more free volumes in the samples, and the dielectric constant and the density also dropped.

Figure 4 shows the relationship between the dielectric constant and density. The best fitted equation giving the highest R^2 value was the polynomial equation, and in Figure 4, the polynomial second-degree equation is plotted with $R^2 = 0.8306$. This relation implies that the second degree lowers the dielectric constant, whereas the first degree lowers the density. The higher the layer number is of the hyperbranched nanocomposite, the lower the density is, and the second degree lowers the dielectric constant. This confirms that a depression in the density yields a lower dielectric constant, and the depression comes from both the hyperbranched polyimide and POSS. The fourth layer of the hyperbranched nanocomposite might possibly continue the lower density and yield an even lower dielectric constant.

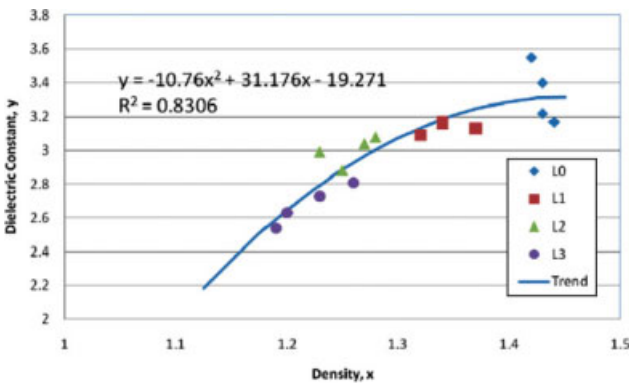

Figure 4 Relationship between the dielectric constant and density. [Color figure can be viewed in the online issue, which is available at www.interscience.wiley.com.]

Morphology of the polyimide and hyperbranched polyimide/POSS nanocomposites

The surface morphologies of the hyperbranched polyimide/POSS nanocomposite and pure polyimide films were investigated with tapping-mode AFM. Figure 5(A,B) displays AFM images of the hyperbranched polyimide/POSS nanocomposite and pure polyimide films, respectively. The degree of surface roughness of the hyperbranched polyimide/POSS nanocomposite and polyimide hybrid film apparently increased with the POSS content. The hyperbranched polyimide/POSS nanocomposites had POSS in their structures; therefore, the roughness of the films containing POSS was greater than that of the pure polyimide films.

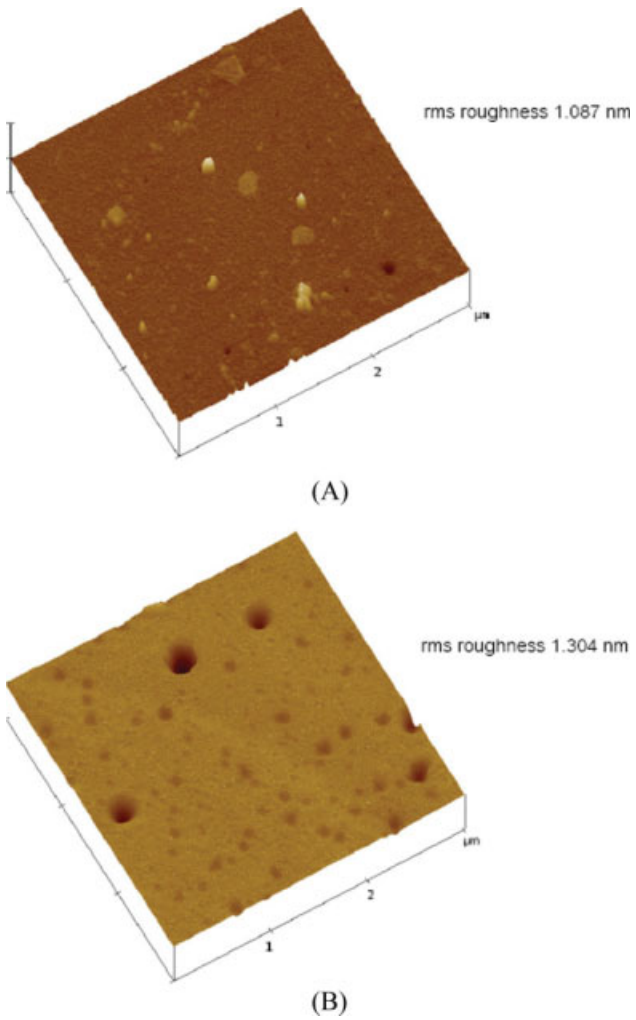

Figure 5 AFM surface analysis of (A) the pure polyimide and (B) PI50–L3 (rms = root mean square). [Color figure can be viewed in the online issue, which is available at www.interscience.wiley.com.]

TABLE V
Solubility of the Pure Polyimide and Various Polyimide Layers

Solvent	Pure polyimide	PI50–L1	PI50–L2	PI50–L3
NMP	oo	oo	oo	oo
DMAc	oo	oo	oo	oo
m-Cresol	o	o	oo	oo
$CHCl_3$	oo	oo	oo	oo
THF	oo	oo	oo	oo
Acetone	oo	oo	oo*	oo*
Toluene	x	x	o	o
Methanol	x	x	x	x
Water	x	x	x	x

o = partially soluble; oo = soluble; oo* = rapidly soluble within 30 min; x = insoluble.

Solubility

In general, the most important properties of hyperbranched polymers versus their linear analogues are higher solubility, low solution viscosity,[11,12] and higher surface reactivity. These improved properties are mainly due to higher branches and denser molecular structures[13] with the larger number of surface groups.

As shown in Table V, the solubility of the polyimide and various layers of the polyimide were determined. The hyperbranched polyimide/POSS nanocomposites had better solubility than the pure polyimide because of the branched structure. This situation was pronounced in toluene, acetone, and *m*-cresol. The higher branch polyimide dissolved easily in comparison with the first layer and the pure polyimide. The polar aprotic solvents NMP and DMAc and normal solvents THF and chloroform could dissolve the polymer, regardless of the degree of branching, and the small-molecule solvents water and methanol could not dissolve the polymer, regardless of the degree of branching.

CONCLUSIONS

Hyperbranched polyimide/POSS nanocomposites were synthesized by the reaction of a bromide-hyperbranched polyether/POSS and a polyimide containing various hydroxyl-functional groups. The reductions in the dielectric constants of the hyperbranched polyimide/POSS nanocomposites can be explained in terms of the free volumes, which were increased by the large POSS structure; this resulted in a loose polyimide matrix because of the hyperbranched structures. The hyperbranched polyimide/POSS nanocomposite possessed lower thermal stability than the pure polyimide film. The densities of the hyperbranched polyimide/POSS nanocomposites corresponded to the dielectric constants. The lower the density was, the higher the free volume was and the lower the dielectric constant was. The experimental results indicated that the hyperbranched polyimide/POSS nanocomposite exhibited increased solubility in comparison with the pure polyimide.

The authors thank Mektec Manufacturing Corp. (Thailand), Ltd., for providing the materials for the polyimide synthesis and the characterization equipment.

References

1. Yuan, J. L.; Jieh, M. H.; Shiao, W. K.; Jian, S. L.; Feng, C. C. Polymer 2005, 46, 173.
2. Chyi, M. L.; Yao, T. C.; Kung, H. W. Chem Mater 2003, 15, 3721.
3. Chyi, M. L.; Reddy, G. M.; Kung, H. W.; Ching, F. S. Chem Mater 2003, 15, 2261.
4. Lichtenhan, J. D.; Vu, N. Q.; Carter, J. A.; Gilman, J. W.; Feher, F. J. Macromolecules 1993, 26, 2141.
5. Lichtenhan, J. D.; Otonari, Y. A.; Carr, M. J. Macromolecules 1995, 28, 8435.
6. Haddad, T. S.; Lichtenhan, J. D. Macromolecules 1996, 29, 7302.
7. Lee, A.; Lichtenhan, J. D. Macromolecules 1970, 31, 4970.
8. Letant, S. E.; Herberg, J.; Dinh, L. N.; Maxwell, R. S.; Simpson, R. L.; Saab, A. P. Catal Commun 2007, 8, 2137.
9. Borah, J.; Karak, N. Polym Int 2004, 53, 2026.
10. Takeichi, T.; Ogura, S.; Takayama, Y. J Polym Sci Part A: Polym Chem 1994, 32, 579.
11. Wooley, K. L.; Frechet, J. M. J.; Hawker, C. J. Polymer 1994, 35, 4489.
12. Hawker, C. J.; Frechet, J. M. J. J Chem Soc Perkin Trans 11992, 2459.
13. Voit, B. J Polym Sci Part A: Polym Chem 2000, 38, 2505.